DOI: 10.1002/ejic.200601114

Syntheses, Structures and Optical Nonlinearities of Heteroselenometallic W–Se–Cu Cluster Compounds Containing Bridging Phosphane Ligands

Zhan Yu,[a] Qian-Feng Zhang,*[a] Yinglin Song,[b] Wai-Yeung Wong,[c] Alexander Rothenberger,[d] and Wa-Hung Leung[e]

Dedicated to Professor Dieter Fenske on the occasion of his 65th birthday

Keywords: Heterometallic complexes / Copper / Selenium / Nonlinear optical properties / Cluster compounds

Treatment of $[Et_4N]_2[WSe_4]$ with the trinuclear trigonal-bipyramidal copper(I) complexes $[Cu_3(\mu_3\text{-}X)_2(\mu\text{-}L)_3]X$ [X = I, L = bis(diphenylphosphanyl)methane (dppm) (**1a**); X = Cl, L = bis(diphenylphosphanyl)amine (dppa) (**1b**)] affords the tetranuclear cluster compounds $[(\mu_3\text{-}WSe_4)Cu_3(\mu\text{-}X)(\mu\text{-}L)_2]$ [X = I, L = dppm (**2a**); X = Cl, L = dppa (**2b**)], which exhibit an open butterfly configuration. Interaction of $[Et_4N]_2[WSe_4]$ with $[Cu(MeCN)_4][PF_6]$ and L gives the pentanuclear cluster compounds $[(\mu_4\text{-}WSe_4)Cu_4(\mu\text{-}L)_4][PF_6]_2$ [L = dppm (**3a**), dppa (**3b**)] which contain an open co-planar WCu_4 core. The solid-state structures of cluster compounds **2a**, **2b**, and **3a** have been established by X-ray crystallography. The nonlinear optical properties of **2a** and **3a** have been examined by z-scan techniques with 7-ns pulses at 532 nm. The pentanuclear co-planar cluster **3a** exhibits a large optical limiting effect (the limiting threshold is about 0.40 J cm^{-2}).
(© Wiley-VCH Verlag GmbH & Co. KGaA, 69451 Weinheim, Germany, 2007)

Introduction

The coordination chemistry of $[MS_4]^{2-}$ anions (M = Mo, W) with transition metal ions has been well developed owing to their relevance to biological systems,[1–3] special optical properties,[4–6] and rich structural variations.[7] However, analogous heterometallic complexes with $[MSe_4]^{2-}$ anions have not been well explored. Heterometallic selenium complexes are of significance, in part, due to their interesting nonlinear optical and electronic properties.[8–10] Studies of the interaction of $[MSe_4]^{2-}$ with the coinage-metal cations, namely Cu^+, Ag^+, and Au^+, have resulted in the isolation of a series of heterometallic selenium clusters with various structural types, including linear, cubane, incomplete cubane, co-planar T-frame and open cross-frame, crown, cage, and pin-wheel shapes, and polymeric frameworks.[11–19] We have a long-standing interest in heterometallic selenium cluster compounds based on the $[MSe_4]^{2-}$ anions.[20] It is noteworthy that the structure of coinage-metal/$[MSe_4]^{2-}$ clusters is closely related to the number of coinage metal ions coordinated to the six MSe_2 edges of the tetrahedral $[MSe_4]^{2-}$ moiety, which depends upon the reaction conditions, especially the M′/$[MSe_4]^{2-}$ (M′ = coinage metal) ratio, and the peripheral ligands.[21] In this context, we report here the synthesis of two types of heterometallic selenium W–Se–Cu cluster compounds, namely tetranuclear butterfly-like $[(\mu_3\text{-}WSe_4)Cu_3(\mu\text{-}I)(\mu\text{-}L)_2]$ [L = dppm (**2a**), dppa (**2b**)] and pentanuclear open co-planar $[(\mu_4\text{-}WSe_4)Cu_4(\mu\text{-}L)_4][PF_6]_2$ [L = dppm (**3a**), dppa (**3b**)], from reactions of tetraselenotungstate anion with copper species in the presence of the bridging phosphane ligands bis(diphenylphosphanyl)methane (dppm) and bis(diphenylphosphanyl)amine (dppa). The nonlinear optical data of the newly prepared heterometallic selenium clusters have been investigated to provide some evidence regarding the structure/property relationships of this class of cluster compounds.

[a] Department of Applied Chemistry, Anhui University of Technology,
Ma'anshan, Anhui 243002, P. R. China
E-mail: zhangqf@ahut.edu.cn
[b] Department of Physics, Harbin Institute of Technology, Harbin 150001, P. R. China
[c] Department of Chemistry, Hong Kong Baptist University, Waterloo Road, Kowloon Tang, Hong Kong, P. R. China
[d] Institut für Anorganische Chemie, Universität Karlsruhe (TH), 76128 Karlsruhe, Germany
[e] Department of Chemistry, The Hong Kong University of Science and Technology,
Clear Water Bay, Kowloon, Hong Kong, P. R. China

Results and Discussion

Syntheses and Spectral Characterizations

It has been reported previously that reactions of copper halides with dppm give a series of trinuclear trigonal-bipyramidal complexes $[Cu_3(\mu_3\text{-}X)_2(\mu\text{-dppm})_3]X$ (X = Cl,[22] Br,[23] I[24]). Similarly, treatment of [CuCl] powder with

 © 2007 Wiley-VCH Verlag GmbH & Co. KGaA, Weinheim

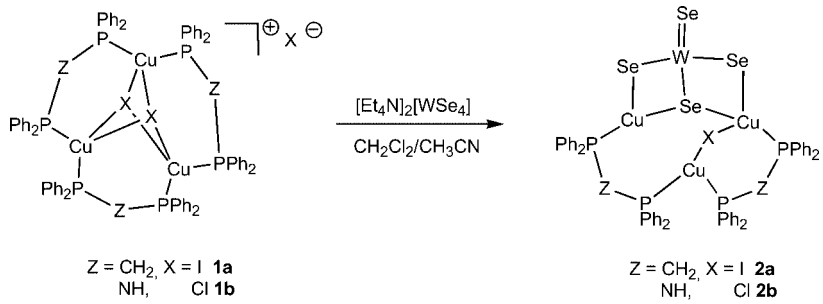

Scheme 1.

1 equiv. of dppa in CH_2Cl_2 affords the complex $[Cu_3(\mu_3\text{-}Cl)_2(\mu\text{-}dppa)_3]Cl$ (**1b**) in nearly quantitative yield. It is therefore not surprising to find a similar behavior between the bridging ligands dppa and dppm in their reaction with copper halides. A similar reaction in thf solution results in the formation of the same cationic complex but with a $[Cu^ICl_2]^-$ anion, which seems to be easily formed in thf.[25] The $^{31}P\{^1H\}$ NMR spectrum of **1b** shows one singlet at δ = 38.2 ppm assignable to the dppa ligands.

The reaction of $[Et_4N]_2[WSe_4]$ with **1a** and **1b** affords the neutral tetranuclear cluster compounds $[(\mu_3\text{-}WSe_4)Cu_3(\mu\text{-}I)(\mu\text{-}dppm)_2]$ (**2a**) and $[(\mu_3\text{-}WSe_4)Cu_3(\mu\text{-}Cl)(\mu\text{-}dppa)_2]$ (**2b**), respectively (Scheme 1). This implies that the formation of **2a** and **2b** involves the metathesis of $[Cu_3(\mu_3\text{-}X)_2(\mu\text{-}L)_3]^+$ (L = dppm and dppa) with the $[WSe_4]^{2-}$ anion. It seems that the displacement of one halide ion and one L molecule from $[Cu_3(\mu_3\text{-}X)_2(\mu\text{-}L)_3]^+$ gives an unsaturated intermediate $[Cu_3(\mu_3\text{-}X)(\mu\text{-}L)_2]^{2+}$, which subsequently coordinates to $[WSe_4]^{2-}$. The trigonal Cu_3 core in these compounds is maintained after the cluster formation, as confirmed by X-ray crystallography (see below). The treatment of $[Et_4N]_2[WSe_4]$ with $[Cu(MeCN)_4][PF_6]$ in the presence of the bidentate phosphane ligands dppm and dppa affords the cationic pentanuclear cluster compounds $[(\mu_4\text{-}WSe_4)Cu_4(\mu\text{-}dppm)_4][PF_6]_2$ (**3a**) and $[(\mu_4\text{-}WSe_4)Cu_4(\mu\text{-}dppa)_4][PF_6]_2$ (**3b**), respectively (Scheme 2). In this reaction, dppm and dppa act as bridging ligands for the construction of a dinuclear $[Cu_2(L)]^{2+}$ species obtained from the 1:1 mixture of $[Cu(MeCN)_4]^-$ and L.[26] Formation of the pentanuclear cluster **3** is not surprising for a co-planar WCu_4 core because the four faces of the tetrahedral $[WSe_4]^{2-}$ anion are equally capable of coordinating to Cu^I species in polar dmf solution. A similar cluster compound $[(\mu_4\text{-}WSe_4)Cu_4(\mu\text{-}dppm)_4][ClO_4]_2$ has been reported previously.[27]

The IR and electronic spectra for **2** and **3** are in agreement with those observed for other known $[WSe_4]^{2-}$ anion derivatives.[11–13,16–19] The W–Se stretching modes of the clusters can be identified as sharp peaks in the low-wavenumber region below 400 cm^{-1}.[11,20,28] The terminal W–Se_t absorptions at 316 cm^{-1} for **2a** and 319 cm^{-1} for **2b** appear at higher wavenumber than the ν(W–Se) absorption (305 cm^{-1} in the $[WSe_4]^{2-}$ anion).[1] The bridging W–Se vibrations are observed in the range 285–300 cm^{-1}, at lower wavenumbers relative to that of $[WSe_4]^{2-}$.[1] The strong absorption at 2011 cm^{-1} in the IR spectrum of **2b** may be attributed to the C≡N stretching vibration of the co-crystallization acetonitrile solvent. The electronic absorption spectrum of each cluster shows several intense bands in the UV region with weaker bands in the visible region (see Figure 1). These bands are not of the d-d type but probably arise from ligand-to-metal charge transfer. Band assignments for heterometallic selenium complexes containing the $[WSe_4]^{2-}$ anion have been reported in the literature.[11–19,28,29] The patterns for both the intense and weaker bands can be assigned to the internal Se-to-W charge-transfer transition of the $[WSe_4]^{2-}$ moiety and a relatively weak ligand $[WSe_4]^{2-}$-to-copper interaction, respectively. It is interesting to note that the $[WSe_4]^{2-}\rightarrow$Cu charge-transfer transition peaks at 470–478 nm in the present clusters are blueshifted by around 20 nm with respect to the $[WSe_4]^{2-}\rightarrow$Ag charge-transfer transition peaks (450–460 nm) in the argentoselenotungstate clusters, while the

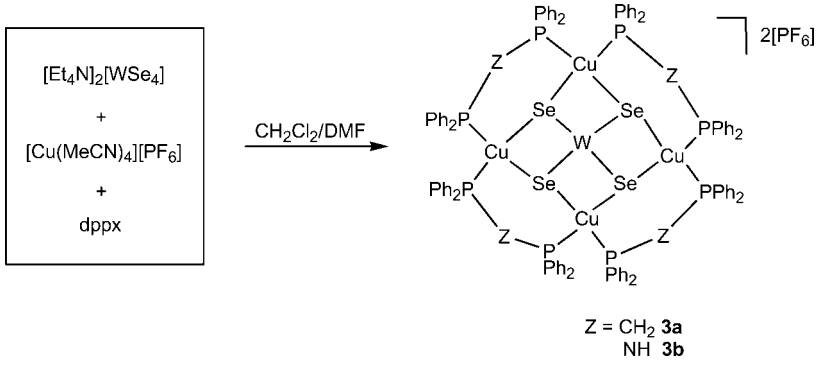

Scheme 2. dppx = dppm for **3a** and dppa for **3b**.

 © 2007 Wiley-VCH Verlag GmbH & Co. KGaA, Weinheim

Se→W charge-transfer peaks at 310–325 nm are less influenced by the different coinage metals in the heteroselenotungstate clusters containing phosphane ligands.[11,18]

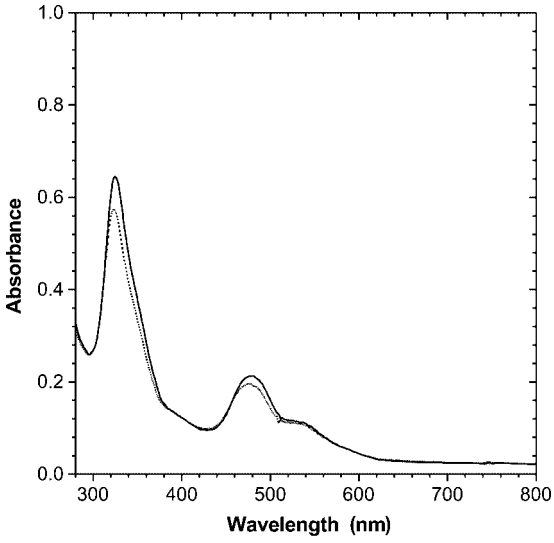

Figure 1. Electronic absorption (UV/Vis) spectra of **2a** (dash) and **2b** (solid), both as 2.75×10^{-4} M CH_2Cl_2 solutions. The optical path is 1 cm.

The $^{31}P\{^1H\}$ NMR spectrum of **2a** shows two singlets at δ = 6.34 and 9.16 ppm, which suggests that there are two magnetically inequivalent phosphorus atoms in the open butterfly cluster. Similarly, two singlets at δ = 41.6 and 47.2 ppm in the ^{31}P NMR spectrum of **2b** may be ascribed to the two phosphorus atoms with different coordination environments. Two ^{31}P signals at δ = 2.57 and –142.5 ppm for **3a** are assigned to the phosphorus atoms of the dppm ligand and $[PF_6]^-$ anion, respectively. Similar ^{31}P signals at δ = 34.3 and –141.2 ppm are observed in the ^{31}P NMR spectrum of **3b**. The FAB^+ mass spectra of compounds **2** and **3** exhibit molecular ions corresponding to $[M^+ + 1]$ and $[M^+ - 2\ [PF_6]^-]$, respectively, with the appropriate isotopic distribution patterns.

Crystal Structures

The structure of **1b**·0.5CH_2Cl_2 comprises a well-separated cation and anion along with the lattice solvent. The molecular structure of the $[Cu_3(\mu_3\text{-}Cl)_2(\mu\text{-}dppa)_3]^+$ cation in **1b** is illustrated in Figure 2, and selected bond lengths and angles are listed in Table 1. Similar to the structures of $[Cu_3(\mu_3\text{-}X)_2(\mu\text{-}dppm)_3]^+$ (X = Cl, Br, I),[22–24] two chloride ions cap the triangle from both sides to form a $[Cu_3Cl_2]$ trigonal bipyramid. Each dppa bidentate ligand bridges one Cu···Cu edge to give a roughly planar $[Cu_3P_6]$ structure. The average distance between two copper atoms in **1b**·0.5CH_2Cl_2 [2.988(2) Å] is slightly shorter than those observed in $[Cu_3(\mu_3\text{-}X)_2(\mu\text{-}dppm)_3]^+$ [X = Cl 3.210(4),[22] Br 3.081(3),[23] I 3.214(2) Å[24]], possibly due to the relatively stronger phosphorus σ-donor of dppa (amide) vs. dppm (methane).[25]

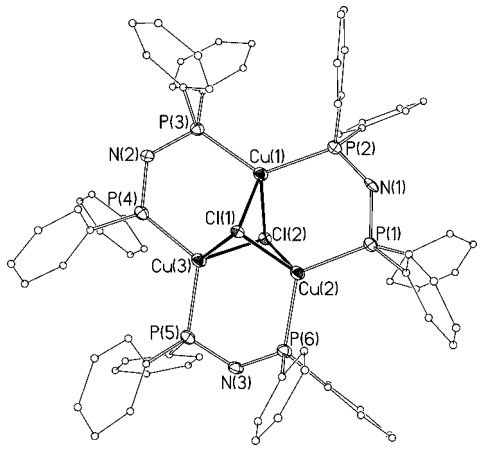

Figure 2. Molecular structure of the $[Cu_3(\mu_3\text{-}Cl)_2(\mu\text{-}dppa)_3]^+$ cation in **1b**.

Table 1. Selected bond lengths [Å] and angles [°] for **1b**·0.5CH_2Cl_2.

Cu(1)–P(2)	2.265(3)	Cu(1)–P(3)	2.274(3)
Cu(2)–P(1)	2.239(3)	Cu(2)–P(6)	2.248(3)
Cu(3)–P(4)	2.236(4)	Cu(3)–P(5)	2.252(3)
Cu(1)–Cl(1)	2.529(3)	Cu(1)–Cl(2)	2.528(3)
Cu(2)–Cl(1)	2.500(3)	Cu(2)–Cl(2)	2.470(3)
Cu(3)–Cl(1)	2.533(2)	Cu(3)–Cl(2)	2.465(3)
Cu(1)···Cu(2)	3.040(2)	Cu(2)···Cu(3)	2.937(2)
P(2)–Cu(1)–P(3)	125.49(12)	P(2)–Cu(1)–Cl(2)	107.32(11)
P(3)–Cu(1)–Cl(2)	113.31(11)	P(2)–Cu(1)–Cl(1)	109.86(11)
P(3)–Cu(1)–Cl(1)	104.50(11)	P(1)–Cu(2)–P(6)	119.64(13)
P(1)–Cu(2)–Cl(2)	108.02(11)	P(6)–Cu(2)–Cl(2)	114.71(11)
P(1)–Cu(2)–Cl(1)	112.07(11)	P(6)–Cu(2)–Cl(1)	106.45(11)
P(4)–Cu(3)–P(5)	119.97(12)	P(4)–Cu(3)–Cl(2)	108.40(11)
P(5)–Cu(3)–Cl(2)	111.05(12)	P(4)–Cu(3)–Cl(1)	108.80(11)
P(5)–Cu(3)–Cl(1)	112.98(11)	Cl(2)–Cu(1)–Cl(1)	90.68(9)
Cl(2)–Cu(2)–Cl(1)	92.71(9)	Cl(2)–Cu(3)–Cl(1)	92.03(9)
Cu(2)–Cl(1)–Cu(1)	74.40(8)	Cu(2)–Cl(1)–Cu(3)	71.39(7)
Cu(1)–Cl(1)–Cu(3)	74.84(7)	Cu(3)–Cl(2)–Cu(2)	73.06(8)
Cu(3)–Cl(2)–Cu(1)	76.05(8)	Cu(2)–Cl(2)–Cu(1)	74.93(8)

The structures of **2a** and **2b**·CH_3CN were also determined by X-ray diffraction. The molecular structures of **2a** and **2b** are shown in Figures 3 and 4, respectively, and selected bond lengths and angles are listed in Tables 2 and 3, respectively. The structural frameworks in both neutral compounds **2a** and **2b** have an open butterfly configuration. The structures of **2a** and **2b**·CH_3CN consist of trigonal $[Cu_3(\mu\text{-}I)(\mu\text{-}dppm)_2]^{2+}$ and $[Cu_3(\mu\text{-}Cl)(\mu\text{-}dppa)_2]^{2+}$ fragments, respectively, that are bound to a tetrahedral $[WSe_4]^{2-}$ moiety. The coordination geometry of the W atom in **2a** or **2b** remains nearly tetrahedral with the Se–W–Se angles ranging from 107.10(12)° to 114.60(15)° in **2a** and from 108.05(8)° to 110.92(10)° in **2b**. The W–Se bond lengths fall into three categories: the W–Se_t, W–μ-Se, and W–μ_3-Se bond lengths are 2.254(3), 2.310(3) (av.), and 2.479(3) Å, respectively, in **2a** [2.251(3), 2.325(3) (av.), and 2.429(2) Å, respectively, in **2b**]. There are three different types of copper atoms in **2**: one has a tetrahedral geometry (bonded to two selenium atoms, one halide ion, and one phosphorus atom) and the other two have a trigonal-planar geometry (one is bonded to two selenium atoms and one

 © 2007 Wiley-VCH Verlag GmbH & Co. KGaA, Weinheim

phosphorus atom, and the other to two phosphorus atoms and one halide ion). The Cu–Se distances in **2** are slightly influenced by the coordination modes of Se and Cu. For example, the Cu–Se distances involving μ-Se and three-coordinate Cu, μ-Se and four-coordinate Cu, μ_3-Se and three-coordinate Cu, and μ_3-Se and four-coordinate Cu are 2.369(4), 2.391(4), 2.396(4), and 2.430(4) Å, respectively, in **2a**. A similar situation is observed in **2b** (see Table 3). The Cu(3)–Se(3) bond in **2a** [2.702(4) Å] and the Cu(3)–Se(4) bond in **2b** [2.742(2) Å] are much longer than those observed in related systems such as $[Cu_4(dppm)_4(\mu_4\text{-Se})][PF_6]_2$ [Cu–μ_4-Se: 2.384(3)–2.387(3) Å][30] and $[Cu_8(\mu_8\text{-Se})\{Se_2P(OiPr)_2\}_6]$ [Cu–μ_8-Se: 2.539(3)–2.624(3) Å],[31] which is indicative of no bonding between the μ_3-Se and $Cu(XP_2)$ moieties. The W···Cu separations for the three-coordinate copper atom [2.718(3) Å in **2a** and 2.698(3) Å in **2b**] are obviously shorter than those for their four-coordinate counterparts [2.779(4) Å in **2a** and 2.780(3) Å in **2b**]. The Cu(1)···Cu(3)···Cu(2) angles of 66.62(11)° in **2a** and 69.30(8)° in **2b** are more obtuse than those in **1a** [60.36(2)°] and **1b** [61.91(5)°], respectively; such an enlargement of the trigonal Cu_3 angles is due to the coordination of $[Cu_3(\mu\text{-}X)(\mu\text{-}L)_2]^{2+}$ species to the $[WSe_4]^{2-}$ anion. Accordingly, the Cu(1)···Cu(3) separations bridged by the halide ion [2.763(4) Å in **2a** and 2.795(3) Å in **2b**] are much shorter than those in **1a** [3.214(2) Å][24] and **1b** [2.988(2) Å], which is suggestive of weak metal–metal interactions between the $[Cu_2(\mu\text{-}X)]$ moieties of the present clusters. The Cu(1)–I(1)–Cu(3) bond angle in **2a** [61.23(10)°] is more acute than the Cu(1)–Cl(1)–Cu(3) bond angle in **2b** [68.95(10)°], whereas the average Cu–I bond in **2a** [2.709(3) Å] is longer than the average Cu–Cl bond in **2b** [2.465(3) Å].

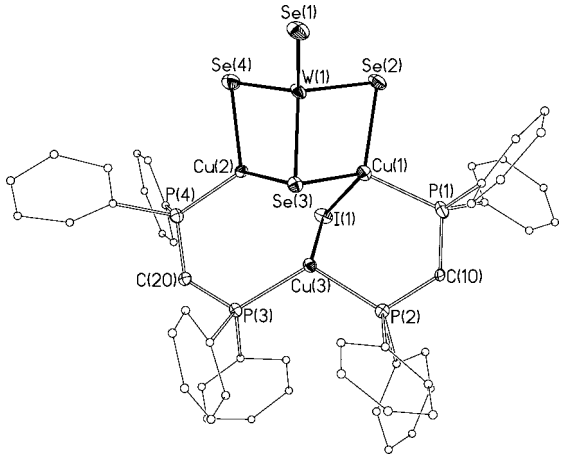

Figure 3. Molecular structure of the $[(\mu_3\text{-}WSe_4)Cu_3(\mu\text{-}I)(\mu\text{-}dppm)_2]$ cation in **2a**.

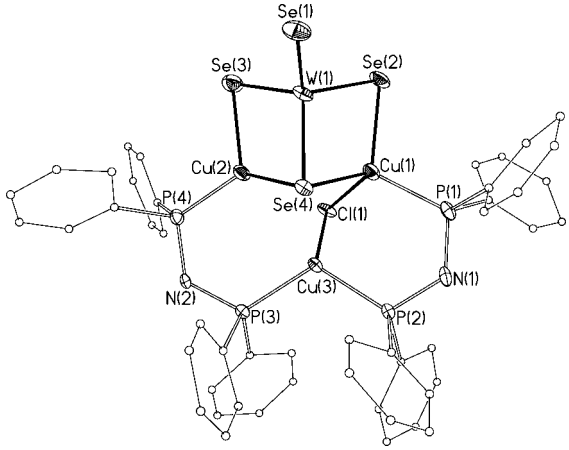

Figure 4. Molecular structure of the $[(\mu_3\text{-}WSe_4)Cu_3(\mu\text{-}Cl)(\mu\text{-}dppa)_2]$ cation in **2b**.

Table 2. Selected bond lengths [Å] and angles [°] for **2a**.

W(1)–Se(1)	2.254(3)	W(1)–Se(2)	2.334(3)
W(1)–Se(3)	2.479(3)	W(1)–Se(4)	2.287(4)
Cu(1)–Se(2)	2.391(4)	Cu(2)–Se(3)	2.396(4)
Cu(1)–Se(3)	2.430(4)	Cu(3)–Se(3)	2.702(4)
Cu(2)–Se(4)	2.369(4)	Cu(1)–I(1)	2.788(4)
Cu(3)–I(1)	2.630(3)	Cu(1)–P(1)	2.214(8)
Cu(2)–P(4)	2.196(7)	Cu(3)–P(3)	2.263(6)
Cu(3)–P(2)	2.271(7)	W(1)···Cu(1)	2.779(4)
W(1)···Cu(2)	2.718(3)	Cu(1)···Cu(3)	2.763(4)
Cu(2)···Cu(3)	3.020(4)		
Se(1)–W(1)–Se(4)	114.60(15)	Se(1)–W(1)–Se(2)	107.25(12)
Se(4)–W(1)–Se(2)	111.40(14)	Se(1)–W(1)–Se(3)	107.10(12)
Se(4)–W(1)–Se(3)	108.53(10)	Se(2)–W(1)–Se(3)	107.67(11)
W(1)–Se(2)–Cu(1)	72.04(11)	W(1)–Se(3)–Cu(2)	67.73(10)
W(1)–Se(3)–Cu(1)	68.95(11)	W(1)–Se(3)–Cu(3)	121.46(11)
Cu(2)–Se(3)–Cu(3)	72.36(11)	Cu(1)–Se(3)–Cu(3)	64.88(11)
P(1)–Cu(1)–Se(2)	107.7(2)	P(1)–Cu(1)–Se(3)	119.1(2)
Se(2)–Cu(1)–Se(3)	107.44(16)	P(1)–Cu(1)–I(1)	106.3(2)
Se(2)–Cu(1)–I(1)	111.88(15)	Se(3)–Cu(1)–I(1)	104.50(13)
P(4)–Cu(2)–Se(4)	112.8(2)	P(4)–Cu(2)–Se(3)	128.8(2)
Se(4)–Cu(2)–Se(3)	108.65(16)	P(3)–Cu(3)–P(2)	117.2(3)
P(3)–Cu(3)–I(1)	107.49(19)	P(2)–Cu(3)–I(1)	113.03(19)
P(3)–Cu(3)–Se(3)	109.30(19)	P(2)–Cu(3)–Se(3)	107.10(19)
I(1)–Cu(3)–Se(3)	101.60(12)	Cu(3)–I(1)–Cu(1)	61.23(10)
Cu(1)···Cu(3)···Cu(2)	66.62(11)		

Table 3. Selected bond lengths [Å] and angles [°] for **2b**·CH_3CN.

W(1)–Se(1)	2.251(3)	W(1)–Se(2)	2.332(2)
W(1)–Se(3)	2.318(3)	W(1)–Se(4)	2.429(2)
Cu(1)–Se(2)	2.377(3)	Cu(2)–Se(3)	2.350(3)
Cu(2)–Se(4)	2.348(3)	Cu(1)–Se(4)	2.425(3)
Cu(3)–Se(4)	2.742(2)	Cu(1)–P(1)	2.194(5)
Cu(2)–P(4)	2.170(5)	Cu(3)–P(3)	2.245(4)
Cu(3)–P(2)	2.264(4)	Cu(1)–Cl(1)	2.570(4)
Cu(3)–Cl(1)	2.359(3)	W(1)···Cu(1)	2.780(3)
W(1)···Cu(2)	2.698(3)	Cu(1)···Cu(3)	2.795(3)
Cu(2)···Cu(3)	3.036(3)		
Se(1)–W(1)–Se(3)	109.58(12)	Se(1)–W(1)–Se(2)	109.98(11)
Se(3)–W(1)–Se(2)	109.52(10)	Se(1)–W(1)–Se(4)	110.92(10)
Se(3)–W(1)–Se(4)	108.76(7)	Se(2)–W(1)–Se(4)	108.05(8)
Se(1)–W(1)–Cu(2)	133.90(12)	W(1)–Se(2)–Cu(1)	72.36(8)
W(1)–Se(3)–Cu(2)	70.61(9)	W(1)–Se(4)–Cu(3)	120.42(7)
W(1)–Se(4)–Cu(2)	68.75(8)	W(1)–Se(4)–Cu(1)	69.86(7)
Cu(2)–Se(4)–Cu(1)	88.17(11)	Cu(2)–Se(4)–Cu(3)	72.76(9)
Cu(1)–Se(4)–Cu(3)	65.15(8)	P(1)–Cu(1)–Se(2)	112.04(15)
P(1)–Cu(1)–Se(4)	118.68(15)	Se(2)–Cu(1)–Se(4)	106.70(11)
P(1)–Cu(1)–Cl(1)	106.89(17)	Se(2)–Cu(1)–Cl(1)	111.27(13)
Se(4)–Cu(1)–Cl(1)	100.69(12)	P(4)–Cu(2)–Se(4)	132.35(17)
P(4)–Cu(2)–Se(3)	112.42(16)	Se(4)–Cu(2)–Se(3)	110.49(12)
P(3)–Cu(3)–P(2)	115.27(16)	P(3)–Cu(3)–Cl(1)	112.95(16)
P(3)–Cu(3)–Se(4)	109.76(13)	P(2)–Cu(3)–Se(4)	105.33(12)
P(2)–Cu(3)–Cl(1)	114.02(16)	Cl(1)–Cu(3)–Se(4)	97.62(11)
Cu(3)–Cl(1)–Cu(1)	68.95(10)	Cu(1)···Cu(3)···Cu(2)	69.30(8)

 © 2007 Wiley-VCH Verlag GmbH & Co. KGaA, Weinheim

The structure of the $[(\mu_4\text{-}WSe_4)Cu_4(\mu\text{-}dppm)_4]^{2+}$ cluster cation in **3a** is shown in Figure 5, and selected bond lengths and angles are listed in Table 4. Similar core structures have been found previously in pentanuclear clusters with a coplanar WCu_4 core, such as the anionic cluster $[Et_4N]_2[(\mu_4\text{-}WSe_4)(CuS_2CNMe_2)_4]$,[32] the neutral cluster $[(\mu_4\text{-}WSe_4)Cu_4Cl_6(py)_4]$[33] (py = pyridine), and the cationic cluster $[(\mu_4\text{-}WSe_4)Cu_4(\mu\text{-}dppm)_4][ClO_4]_2$.[27] The W atom is at the center of a slightly distorted tetrahedral WSe_4 unit with an average W–Se bond length of 2.347(1) Å and Se–W–Se angles in the range 105.44(3)–111.85(3)°. Four copper atoms are almost symmetrically bound to the four WSe_2 edges of the tetrahedral $[WSe_4]^{2-}$ anion. Four distorted chair-type six-membered CP_2Cu_2Se rings around the $[WSe_4]^{2-}$ anion enhance the structural stability of the cationic cluster **3a**. The five metal atoms in the WCu_4 core are nearly coplanar with deviations of not more than 0.01 Å from the least-squares plane. The average W–Cu distance of 2.820(1) Å in **3a** is similar to those in $[(\mu_4\text{-}WSe_4)Cu_4(\mu\text{-}dppm)_4][ClO_4]_2$ [2.815(2) Å][27] and $(\mu_2\text{-}WSe_4)[Cu(PMe_2Ph)_2]_2$ [2.873(2) Å], which contain σ-donor phosphane ligands,[11] but clearly longer than those in $[Et_4N]_2[(\mu_3\text{-}WSe_4)(CuS_2CNEt_2)_3]$ [av. 2.737(2) Å] and $[Et_4N]_2[(\mu_4\text{-}WSe_4)(CuS_2CNMe_2)_4]$ [av. 2.707(2) Å], which contain π-conjugated dithiocarbamate ligands.[32]

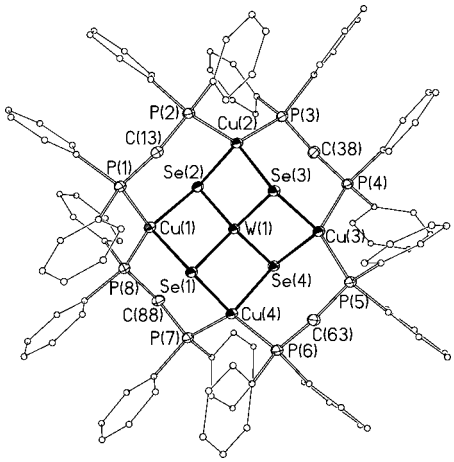

Figure 5. Molecular structure of the $[(\mu_4\text{-}WSe_4)Cu_4(\mu\text{-}dppm)_4]^{2+}$ cation in **3a**.

Table 4. Selected bond length [Å] and angles [°] for **3a**.

W(1)–Se(1)	2.3490(8)	W(1)–Se(2)	2.3490(12)
W(1)–Se(3)	2.3456(9)	W(1)–Se(4)	2.3457(8)
Cu(1)–Se(1)	2.4594(14)	Cu(1)–Se(2)	2.4461(10)
Cu(2)–Se(2)	2.4617(12)	Cu(2)–Se(3)	2.4520(14)
Cu(3)–Se(3)	2.4523(10)	Cu(3)–Se(4)	2.4458(11)
Cu(4)–Se(4)	2.4560(10)	Cu(4)–Se(1)	2.4317(10)
Cu(1)–P(1)	2.2763(16)	Cu(1)–P(8)	2.2667(18)
Cu(2)–P(2)	2.2697(16)	Cu(2)–P(3)	2.2676(17)
Cu(3)–P(4)	2.2663(16)	Cu(3)–P(5)	2.2656(18)
Cu(4)–P(6)	2.2662(19)	Cu(4)–P(7)	2.2729(18)
W(1)···Cu(1)	2.8096(12)	W(1)···Cu(2)	2.8357(14)
W(1)···Cu(3)	2.8075(12)	W(1)···Cu(4)	2.8285(14)
Se(3)–W(1)–Se(4)	111.77(4)	Se(3)–W(1)–Se(1)	105.44(3)
Se(4)–W(1)–Se(1)	110.81(4)	Se(3)–W(1)–Se(2)	111.24(4)
Se(4)–W(1)–Se(2)	105.85(3)	Se(1)–W(1)–Se(2)	111.85(3)
W(1)–Se(1)–Cu(4)	72.53(4)	W(1)–Se(1)–Cu(1)	71.47(3)
W(1)–Se(2)–Cu(1)	71.70(3)	W(1)–Se(2)–Cu(2)	72.19(4)
W(1)–Se(3)–Cu(2)	72.43(4)	W(1)–Se(3)–Cu(3)	71.59(4)
W(1)–Se(4)–Cu(3)	71.70(4)	W(1)–Se(4)–Cu(4)	72.14(4)
Cu(4)–Se(1)–Cu(1)	108.15(4)	Cu(1)–Se(2)–Cu(2)	109.89(4)
Cu(2)–Se(3)–Cu(3)	108.75(4)	Cu(3)–Se(4)–Cu(4)	108.97(4)
Se(2)–Cu(1)–Se(1)	104.98(4)	Se(3)–Cu(2)–Se(2)	104.10(4)
Se(4)–Cu(3)–Se(3)	104.92(4)	Se(1)–Cu(4)–Se(4)	104.49(4)
P(8)–Cu(1)–P(1)	132.26(7)	P(8)–Cu(1)–Se(2)	105.80(5)
P(1)–Cu(1)–Se(2)	107.49(6)	P(8)–Cu(1)–Se(1)	104.86(5)
P(1)–Cu(1)–Se(1)	98.46(5)	P(3)–Cu(2)–P(2)	131.77(6)
P(3)–Cu(2)–Se(3)	106.99(5)	P(2)–Cu(2)–Se(3)	103.06(5)
P(3)–Cu(2)–Se(2)	104.64(5)	P(2)–Cu(2)–Se(2)	103.49(6)
P(5)–Cu(3)–P(4)	128.05(7)	P(5)–Cu(3)–Se(4)	105.33(6)
P(4)–Cu(3)–Se(4)	105.81(6)	P(5)–Cu(3)–Se(3)	108.20(5)
P(4)–Cu(3)–Se(3)	102.56(5)	P(6)–Cu(4)–P(7)	127.67(6)
P(6)–Cu(4)–Se(1)	105.65(5)	P(7)–Cu(4)–Se(1)	105.17(6)
P(6)–Cu(4)–Se(4)	103.06(6)	P(7)–Cu(4)–Se(4)	108.76(5)

NLO Properties

The nonlinear absorption component of cluster compounds **2a** and **3a** was evaluated by a *z*-scan experiment in an open-aperture configuration (see Figure 6). Although the detailed mechanism is still not clear, it is interesting to note that the NLO absorption data obtained under the conditions used in this study can be well described by Equations (1) and (2), which describe a third-order NLO process, where α_0 and α_2^{eff} are the linear and effective third-order NLO absorptivities, respectively.[34,35]

$$T(Z) = \{1/[\pi^{1/2}q(Z)]\}\int_{-\infty}^{\infty}\ln[1 + q(Z)]e^{-\tau^2}d\tau \quad (1)$$

$$q(Z) = \alpha_2^{eff}I_0[(1 - e^{-\alpha_0 L})/\alpha_0] \quad (2)$$

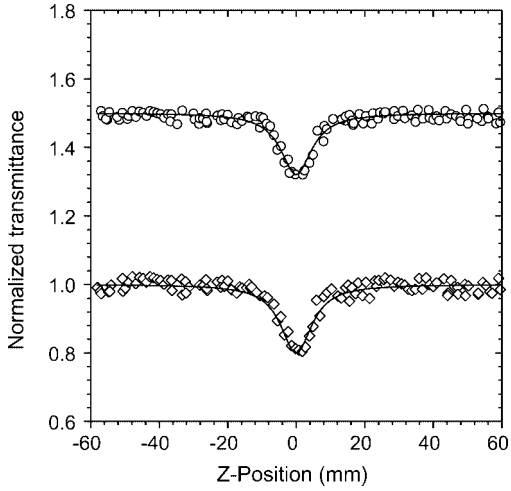

Figure 6. *z*-Scan data of cluster compounds **2a** (circle) and **3a** (diamond) in 2.75×10^{-4} M CH_2Cl_2 solution. The data were collected in an open-aperture configuration. The solid curves are fits based on theoretical calculations.

The best fit of the theoretical curve (the solid curve in Figure 6) to the experimental data clearly illustrates that the absorption increases as the incident light irradiance arises, which is characteristic of a reverse saturable absorption (RSA) process.[34] The origin of the observed RSA in cluster

 © 2007 Wiley-VCH Verlag GmbH & Co. KGaA, Weinheim

compounds **2a** and **3a** can be attributed to excited-state absorption. Figure 7 shows the *z*-scan data measured with the aperture and indicates that the two cluster compounds **2a** and **3a** have a negative sign for the refractive nonlinearity, which gives rise to self-defocusing. The measurements confirm that the observed NLO effects are effectively third-order in nature, which implies that both the absorption coefficient and refractive index should be expressed as $\alpha = \alpha_0 + \alpha_2 I$ and $n = n_0 + n_2 I$, respectively, where α_0 and α_2 are the linear and nonlinear absorption coefficients and n_0 and n_2 are the linear and nonlinear refractive indices, respectively, and I is the irradiance of the laser beam within the sample. By applying the *z*-scan theory, the solid curves in Figures 6 and 7 can be fitted to the experimental data. The best fits reveal that $\alpha_2 = 1.74 \times 10^{-6}\ m\,W^{-1}\,M^{-1}$ and $n_2 = -5.32 \times 10^{-13}\ m^2\,W^{-1}\,M^{-1}$ for cluster **2a**, and $\alpha_2 = 2.56 \times 10^{-6}\ m\,W^{-1}\,M^{-1}$ and $n_2 = -1.54 \times 10^{-12}\ m^2\,W^{-1}\,M^{-1}$ for cluster **3a**.

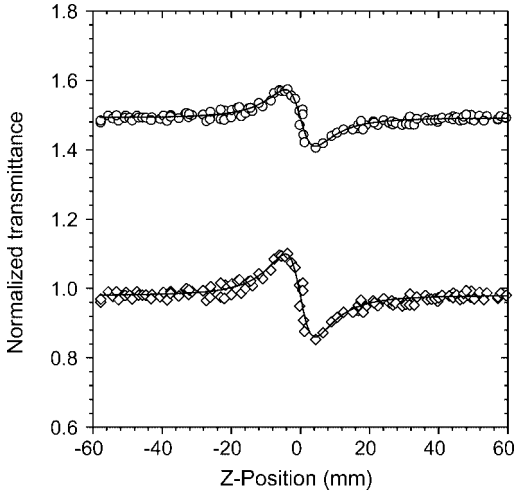

Figure 7. *z*-Scan data of cluster compounds **2a** (circle) and **3a** (diamond) in 2.75×10^{-4} M CH_2Cl_2 solution. The data were obtained by dividing the normalized *z*-scan data obtained in a closed-aperture configuration by the normalized *z*-scan data obtained in an open-aperture configuration. The solid curves are fits based on theoretical calculations.

The optical limiting effects of cluster compounds **2a** and **3a** are depicted in Figure 8. At very low fluences, they respond linearly to the incident light and therefore obey Beer's law. Deviation from the linear response takes place when the incident fluence reaches about 0.35 $J\,cm^{-2}$ for **2a** and 0.12 $J\,cm^{-2}$ for **3a**. The cluster materials become increasingly less transparent as the light fluence rises. Experiments with the solvents alone showed no detectable optical limiting effect. These observations indicate that solvent contributions are negligible. The limiting threshold, which is defined as the incident fluence at which the actual transmittance falls to 55% of the corresponding linear transmittance, was found to be 1.2 $J\,cm^{-2}$ for **2a** and 0.4 $J\,cm^{-2}$ for **3a**. Cluster **2a**, which has a butterfly configuration, therefore has a higher threshold than that of cluster **3a**, which has an open co-planar WCu_4 core, an obvious indication of the influence of structural types on the non-linear optical properties. The butterfly-shaped clusters have two different types of coordinated selenium atoms, therefore the electronic interactions between μ-Se- and μ_3-Se-bridged metal atoms may result in different electron delocalization in the cluster molecule, which needs a higher pump energy to generate the plasma and further leads to degradation of the limiting effect.[36] Similar to the butterfly-shaped clusters, the clusters of other structural types, including incomplete cubane-like, T-frame, and nest-shapes with non-equivalent bridging selenium or sulfur atoms, have lower optical limiting effects.[32,37,38] Previous reports have shown that cluster compounds with an open co-planar cross MCu_4 (M = Mo, W) core, for example the neutral clusters $[(\mu_4\text{-}MS_4)Cu_4(SCN)_2(py)_6]$ (0.3 $J\,cm^{-2}$)[39] and $[(\mu_4\text{-}MS_4)Cu_4(CN)_2(py)_6]$ (0.1 $J\,cm^{-2}$),[40] the anionic clusters $[\{Et_4N\}_2\{(\mu_4\text{-}MS_4)Cu_4(CN)_4\}]_n$ (0.2 $J\,cm^{-2}$)[41] and $[\{Et_4N\}_2\{(\mu_4\text{-}WSe_4)Cu_4(CN)_4\}]_n$ (0.3 $J\,cm^{-2}$),[18] and the cationic clusters $[(\mu_4\text{-}WSe_4)Cu_4(\mu\text{-}dppm)_4][ClO_4]_2$ (0.35 $J\,cm^{-2}$), have a large optical limiting effect.[27] These clusters have four equivalent μ_4-Se atoms, therefore the plasma in the polarized nanosecond pulses may be generated at a lower pump energy, and lower limiting thresholds are therefore found for this class of clusters.[42] The lower limiting threshold of cluster compound **3a** (0.40 $J\,cm^{-2}$) may provide effective proof for this class of clusters that possess an open co-planar structure.

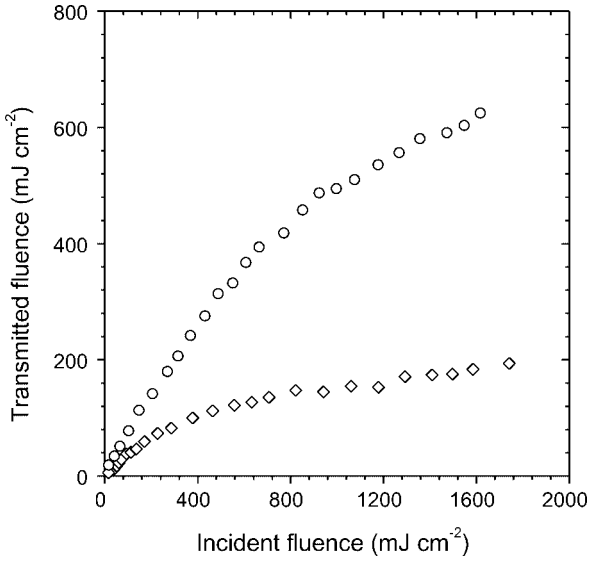

Figure 8. Optical limiting effect of cluster compounds **2a** (circle) and **3a** (diamond) in 2.75×10^{-3} M CH_2Cl_2 solution.

Conclusion

We have investigated the reaction of the anion $[WSe_4]^{2-}$ with copper(I) species in the presence of bridging phosphane ligands dppm and dppa and have isolated two types of heterometallic selenium cluster compounds, namely tetranuclear, butterfly-like $[(\mu_3\text{-}WSe_4)Cu_3(\mu\text{-}X)(\mu\text{-}L)_2]$ and pentanuclear, open co-planar $[(\mu_4\text{-}WSe_4)Cu_4(\mu\text{-}L)_4][PF_6]_2$ (X = Cl, I; L = dppm, dppa). The open co-planar cluster with a WCu_4 core structure has a relatively large optical

 © 2007 Wiley-VCH Verlag GmbH & Co. KGaA, Weinheim

limiting effect and therefore may be considered as a promising candidate for a nonlinear optical limiting cluster material. We are currently investigating the design and synthesis of new heterometallic selenium clusters with strong NLO properties.

Experimental Section

General: All reactions were performed using Schlenk techniques under nitrogen. $[Et_4N]_2[WSe_4]$[43] and $[Cu_3(\mu_3\text{-}I)_2(\mu\text{-}dppm)_3]I$[24] (**1a**) were prepared according to literature methods. $[Cu(MeCN)_4][PF_6]$ was synthesized by the reaction of Cu_2O powder with HPF_6 in acetonitrile.[44] Bis(diphenylphosphanyl)amine (dppa) was synthesized by the reaction of Ph_2PCl with $(Me_3Si)NH(SiMe_3)$ in toluene.[45] CuI and bis(diphenylphosphanyl)methane (dppm) were purchased from Aldrich Ltd. and used without further purification. IR spectra were recorded with a Digilab FTS-40 spectrophotometer. Electronic spectra were recorded with a Hitachi U-3410 spectrophotometer. NMR spectra were recorded with a Bruker ALX 300 spectrometer operating at 300 and 121.5 MHz for ^1H and ^{31}P, respectively; chemical shifts (δ in ppm) are quoted relative to $SiMe_4$ (^1H) and H_3PO_4 (^{31}P). Mass spectra were recorded with a Finnigan TSQ 7000 spectrometer. All elemental analyses were performed with a Perkin–Elmer 2400 CHN analyzer.

$[Cu_3(\mu_3\text{-}Cl)_2(\mu\text{-}dppa)_3]Cl$ (1b): A mixture of CuCl powder (150 mg, 0.15 mmol) and dppa (578 mg, 0.15 mmol) in CH_2Cl_2 (20 mL) was stirred at room temperature overnight. The resulting colorless solution was filtered and the volume of filtrate was reduced to about 10 mL. Colorless block crystals of $[Cu_3(\mu_3\text{-}Cl)_2(\mu\text{-}dppa)_3]Cl$ (**1b**) were obtained by layering hexane on top of the filtrate at room temperature. Yield: 746 mg (96%). IR (KBr): $\tilde{\nu}$ = 3335 [br ν(N–H)]; 531 (s), 509 (s), 492 (m) [ν(P–C)] cm^{-1}. ^1H NMR ($CDCl_3$): δ = 8.05 (br., 3 H, N*H*), 7.21–7.52 (m, 60 H, Ph) ppm. $^{31}P\{^1H\}$ NMR ($CDCl_3$): δ = 37.2 (s) ppm. MS (FAB): *m*/*z* = 1414 $[Cu_3(\mu_3\text{-}Cl)_2(\mu\text{-}dppa)_3]^+$, 512 $[[Cu_2(\mu\text{-}dppa)]^+ - 1]$. $C_{72}H_{63}Cl_2Cu_3N_3P_6\cdot 0.5CH_2Cl_2$ (1495.5): calcd. C 58.2, H 4.28, N 2.81; found C 57.7, H 4.15, N, 2.78.

$[(\mu_3\text{-}WSe_4)Cu_3(\mu\text{-}I)(\mu\text{-}dppm)_2]$ (2a): A solution of **1a** (346 mg, 0.25 mmol) in CH_2Cl_2 (15 mL) was added to a solution of $[Et_4N]_2[WSe_4]$ (152 mg, 0.20 mmol) in dmf (5 mL). After stirring at room temperature for 45 min, the mixture was filtered through a filter paper to provide an orange filtrate. Slow addition of Et_2O resulted in the formation of orange block crystals suitable for single-crystal X-ray diffraction analysis, which were subsequently identified as **2a**. Yield: 183 mg (52%). UV/Vis (CH_2Cl_2): λ_{max} (ε) = 315 (6.94×10^{-3}), 475 (2.91×10^{-3} $M^{-1}cm^{-1}$) nm. IR (KBr): $\tilde{\nu}$ = 312 (s), 295 (m), 291 (w) [ν(W–Se)] cm^{-1}. ^1H NMR ($CDCl_3$): δ = 7.33–7.51 (m, 40 H, Ph), 5.42 (s, 4 H, CH_2) ppm. ^{31}P NMR ($CDCl_3$): δ = 6.34, 9.16 ppm. MS (FAB): *m*/*z* = 1587 $[M^+ + 1]$. $C_{50}H_{44}Cu_3I_2P_4Se_4W$ (1585.9): calcd. C 37.8, H 2.77; found C 37.3, H 2.76.

$[(\mu_3\text{-}WSe_4)Cu_3(\mu\text{-}Cl)(\mu\text{-}dppa)_2]$ (2b): This compound was prepared similarly to **2a** but using **1b** (291 mg, 0.20 mmol) instead of **1a**. It was recrystallized from CH_2Cl_2/MeCN/Et_2O. Yield: 168 mg (46%). UV/Vis (CH_2Cl_2): λ_{max} (ε) = 318 (5.63×10^{-3}), 472 (3.04×10^{-3} $M^{-1}cm^{-1}$) nm. IR (KBr): $\tilde{\nu}$ = 311 (s), 298 (m), 292 (w) [ν(W–Se)] cm^{-1}. ^1H NMR ($CDCl_3$): δ = 7.84 (br., 2 H, N*H*), 7.23–7.45 (m, 40 H, Ph) ppm. ^{31}P NMR ($CDCl_3$): δ = 41.6, 47.2 ppm. MS (FAB): *m*/*z* = 1496 $[M^+ + 1]$. $C_{48}H_{41}ClCu_3N_2P_4Se_4W\cdot CH_3CN$ (1536.5): calcd. C 39.0, H 2.86, N 2.73; found C 38.1, H 2.74, N 2.71.

$[(\mu_4\text{-}WSe_4)Cu_4(\mu\text{-}dppm)_4][PF_6]_2$ (3a): A mixture of $[Cu(MeCN)_4][PF_6]$ (300 mg, 0.80 mmol) and dppm (320 mg, 0.80 mmol) in CH_2Cl_2 (20 mL) was added to a solution of $[Et_4N]_2[WSe_4]$ (152 mg, 0.20 mmol) in dmf (10 mL). After stirring at room temperature for 45 min, the mixture was filtered through a filter paper to provide an orange-red filtrate. Slow addition of Et_2O afforded red block-shaped crystals suitable for a single-crystal X-ray diffraction analysis, which were subsequently identified as **3a**. Yield: 279 mg (73%). UV/Vis (CH_2Cl_2): λ_{max} (ε) = 324 (6.62×10^{-3}), 478 (3.06×10^{-3} $M^{-1}cm^{-1}$) nm. IR (KBr): $\tilde{\nu}$ = 312 (s), 297 (m), 290 (w) [ν(W–Se)] cm^{-1}. ^1H NMR ($CDCl_3$): δ = 7.16–7.52 (m, 80 H, Ph), 5.42 (s, 8 H, C*H*$_2$) ppm. ^{31}P NMR ($CDCl_3$): δ = 2.57, –142.5 ppm. MS (FAB): *m*/*z* 2291 $[M^+ - 2\ PF_6]$. $C_{100}H_{88}Cu_4F_{12}P_{10}Se_4W$ (2581.3): calcd. C 46.5, H 3.41; found C 46.2, H 3.37.

$[(\mu_4\text{-}WSe_4)Cu_4(\mu\text{-}dppa)_4][PF_6]_2$ (3b): This compound was prepared similarly to **3a** but using dppa (320 mg, 0.80 mmol) instead of dppm. It was recrystallized from CH_2Cl_2/MeCN/Et_2O. Yield: 184 mg (49%). UV/Vis (CH_2Cl_2): λ_{max} (ε) = 319 (6.82×10^{-3}), 473 (2.75×10^{-3} $M^{-1}cm^{-1}$) nm. IR (KBr): 313 (s), 298 (m), 294 (w) [ν(W–Se)] cm^{-1}. ^1H NMR ($CDCl_3$): δ = 8.06 (br., 4 H, N*H*), 7.32–7.57 (m, 80 H, Ph) ppm. ^{31}P NMR ($CDCl_3$): δ = 34.3, –141.2 ppm. MS (FAB): *m*/*z* = 2290 $[M^+ - 2\ PF_6]$. $C_{96}H_{84}Cu_4F_{12}N_4P_{10}Se_4W$ (2585.2): calcd. C 44.6, H 3.25, N 2.17; found C 44.2, H 3.18, N 2.13.

Crystal Structure Determination: Data for **1b**·$0.5CH_2Cl_2$ were collected at 293 K with a Bruker SMART-CCD area detector diffractometer with a graphite monochromator using Mo-K_α radiation (λ = 0.71073 Å). Data for **2a**, **2b**·CH_3CN, and **3a** were collected at 153 K with a Siemens Stoe-IPDS diffractometer (Mo-K_α radiation; λ = 0.71073 Å) equipped with an imaging plate area detector and a rotating anode. The intensities were corrected for Lorentz, polarization, and absorption effects. The structures were solved by direct methods using the SHELXTL software package.[46] The positions of all W, Se, Cu, I (Cl), and P atoms were revealed on the first refinement. Other non-hydrogen atoms were located from subsequent difference Fourier syntheses. The structures were refined by full-matrix least-squares methods on F^2. All non-hydrogen atoms were refined anisotropically. Hydrogen atoms were included but not refined. Two of the phenyl rings of the dppm ligands in **2b**·CH_3CN were refined with bond-length restraints due to disorder. Further details of the structure analyses are given in Table 5. CCDC-628300 (**1b**·$0.5CH_2Cl_2$), -628301 (**2a**), -628302 (**2b**·CH_3CN), and -628303 (**3a**) contain the supplementary crystallographic data for this paper. These data can be obtained free of charge from The Cambridge Crystallographic Data Centre via www.ccdc.cam.ac.uk/data_request/cif.

Optical Measurements: A CH_2Cl_2 solution of cluster **2a** or **3a** was placed in a 1-mm quartz cuvette for nonlinear optical measurements, which were performed with linearity polarized 7-ns pulses at 532 nm generated from a Q-switched frequency-doubled Nd:YAG laser. Both clusters are stable toward air and laser light under these conditions. The spatial profiles of the pulsed laser were focused on the sample cell with a 30-cm focal length mirror. The spot radius of the laser beam was measured to be 55 μm (half-width at $1/e^2$ maximum). The incident and transmitted pulse energies were measured simultaneously with two energy detectors (Laser Precision Rjp-735), which were linked to a computer by an IEEE interface.[34,35] The NLO properties of the samples were manifested by moving the samples along the axis of the incident laser irradiance beam (*z*-direction) with respect to the focal point and with the incident laser irradiance kept constant (*z*-scan methods). The closed-aperture curves are normalized to the open-aperture curves. An

 © 2007 Wiley-VCH Verlag GmbH & Co. KGaA, Weinheim

Table 5. Crystal data and structure refinement for $[Cu_3(\mu_3\text{-}Cl)_2(\mu\text{-}dppa)_3]Cl\cdot 0.5CH_2Cl_2$ (**1b**·$0.5CH_2Cl_2$), $[(\mu_3\text{-}WSe_4)Cu_3(\mu\text{-}I)(\mu\text{-}dppm)_2]$ (**2a**), $[(\mu_3\text{-}WSe_4)Cu_3(\mu\text{-}Cl)(\mu\text{-}dppa)_2]\cdot CH_3CN$ (**2b**·CH_3CN), and $[(\mu_4\text{-}WSe_4)Cu_4(\mu\text{-}dppm)_4][PF_6]_2$ (**3a**).

Compound	**1b**·$0.5CH_2Cl_2$	**2a**	**2b**·CH_3CN	**3a**
Formula	$C_{72.5}H_{64}N_3Cl_4P_6Cu_3$	$C_{50}H_{44}P_4ICu_3Se_4W$	$C_{50}H_{44}N_3ClP_4Cu_3Se_4W$	$C_{100}H_{88}F_{12}P_{10}Cu_4Se_4W$
Formula weight	1495.51	1585.94	1536.52	2581.25
Crystal system	triclinic	monoclinic	monoclinic	triclinic
Space group	$P\bar{1}$	$P2_1/c$	$P2_1/c$	$P\bar{1}$
a [Å]	13.5358(17)	18.878(4)	18.094(4)	15.048(3)
b [Å]	14.4773(18)	14.238(3)	14.237(3)	15.268(3)
c [Å]	20.357(3)	21.255(4)	21.249(4)	25.010(5)
α [°]	76.984(7)	90	90	78.97(3)
β [°]	75.046(7)	108.90(3)	103.82(3)	83.64(3)
γ [°]	87.325(7)	90	90	62.96(3)
V [Å^3]	3754.9(8)	5405.1(19)	5315.4(18)	5021.3(17)
Z	2	4	4	2
$D_{calcd.}$ [g cm^{-3}]	1.323	1. 949	1.920	1.707
Temperature [K]	293(2)	153(2)	153(2)	153(2)
F(000)	1530	3016	3128	2544
μ(Mo-K_α) [mm^{-1}]	1.153	6.075	6.288	3.652
No. reflections measured	47388	41609	35233	40271
No. unique reflections	13181	11652	10417	20409
No. observed reflections	7262	9239	7779	16200
No. parameters	806	568	551	1180
R_{int}	0.0722	0.0571	0.0605	0.0687
R_1,[a] wR_2[b] [$I \geq 2\sigma(I)$]	0.0753, 0.1342	0.0618, 0.0901	0.0690, 0.0956	0.0480, 0.1297
R_1,[a] wR_2[b] (all data)	0.0971, 0.2133	0.0828, 0.1455	0.1021, 0.1549	0.0624, 0.1450
GoF[c]	1.097	1.012	1.043	1.073
Final diff. peaks [e Å^{-3}]	+1.015, –1.060	+1.778, –1.669	+1.147, –1.229	+1.946, –1.493

[a] $R_1 = ||F_o| - |F_c||/|F_o|$. [b] $wR_2 = [w(|F_o^2| - |F_c^2|)^2/w|F_o^2|^2]^{1/2}$. [c] GoF = $[w(|F_o| - |F_c|)2/(N_{obs} - N_{param})]^{1/2}$.

aperture of 0.2 mm radius was placed in front of the detector to measure the transmitted energy when assessment of laser beam distortion was needed. To eliminate scattering effects, a lens was mounted after the samples to collect the scattered light.

Acknowledgments

This project was supported by the Natural Science Foundation of China (project number 90301005) and the Hong Kong Research Grants Council (project number 601506). Q.-F. Z. would like to thank the Science and Technological Fund of Anhui Province for Outstanding Youth (06046100) and the Research Fund for the Returned Overseas Talents of Anhui Province (2006Z041).

[1] A. Müller, E. Diemann, R. Jostes, H. Bögge, *Angew. Chem. Int. Ed. Engl.* **1981**, *20*, 934–954.
[2] D. Coucouvanis, *Acc. Chem. Res.* **1991**, *24*, 1–73.
[3] R. H. Holm, *Adv. Inorg. Chem.* **1992**, *38*, 1–71.
[4] S. Shi, W. Ji, S. H. Tang, J. P. Lang, X. Q. Xin, *J. Am. Chem. Soc.* **1994**, *116*, 3615–3616.
[5] C.-M. Che, B.-H. Xia, J.-S. Huang, C.-K. Chan, Z.-Y. Zhou, K.-K. Cheung, *Chem. Eur. J.* **2001**, *7*, 3998–4006.
[6] B. J. Coe, in *Comprehensive Coordination Chemistry II* (Eds.: J. A. McCleverty, T. J. Meyer), Elsevier Pergamon, Oxford, U.K., **2004**, vol. 9, pp. 621–687.
[7] X. T. Wu, P. C. Chen, S. W. Du, Z. Y. Zhu, J. X. Lu, *J. Cluster Sci.* **1994**, *5*, 265–276.
[8] Q. F. Zhang, Y. N. Xiong, T. S. Lai, W. Ji, X. Q. Xin, *J. Phys. Chem. B* **2000**, *104*, 3476–3479.
[9] B. J. Coe, N. R. M. Curati, *Comments Inorg. Chem.* **2004**, *25*, 147–184.
[10] J. Wachter, *Eur. J. Inorg. Chem.* **2004**, 1367–1378.
[11] C. C. Christuk, M. A. Ansari, J. A. Ibers, *Inorg. Chem.* **1992**, *31*, 4365–4369.
[12] R. J. Salm, J. A. Ibers, *Inorg. Chem.* **1994**, *33*, 4216–4220.
[13] Q. M. Wang, X. T. Wu, Q. Huang, T. L. Sheng, P. Lin, *Polyhedron* **1997**, *16*, 1439–1443.
[14] M. C. Hong, M. H. Wu, X. Y. Huang, F. L. Jiang, R. Cao, H. Q. Liu, J. X. Lu, *Inorg. Chim. Acta* **1997**, *260*, 73–77.
[15] M. C. Hong, Q. F. Zhang, R. Cao, D. X. Wu, J. T. Chen, W. J. Zhang, H. Q. Liu, J. X. Lu, *Inorg. Chem.* **1997**, *36*, 6251–6260.
[16] C. C. Christuk, M. A. Ansari, J. A. Ibers, *Angew. Chem. Int. Ed. Engl.* **1992**, *31*, 1477–1478.
[17] Q. F. Zhang, Z. Yu, J. Ding, Y. Song, A. Rothenberger, D. Fenske, W. H. Leung, *Inorg. Chem.* **2006**, *45*, 5187–5195.
[18] Q. F. Zhang, J. Ding, Z. Yu, Y. Song, A. Rothenberger, D. Fenske, W. H. Leung, *Inorg. Chem.* **2006**, *45*, 8638–8647.
[19] Q. F. Zhang, W. H. Leung, X. Q. Xin, H. K. Fun, *Inorg. Chem.* **2000**, *39*, 417–516.
[20] Q. F. Zhang, W. H. Leung, X. Q. Xin, *Coord. Chem. Rev.* **2002**, *224*, 35–49.
[21] Y. Y. Niu, H. G. Zheng, H. W. Hou, X. Q. Xin, *Coord. Chem. Rev.* **2004**, *248*, 169–183.
[22] N. Bresciani, N. Marsich, G. Nardin, L. Randaccio, *Inorg. Chim. Acta* **1974**, *10*, L5–L6.
[23] J. K. Bera, M. Nethaji, A. G. Samuelson, *Inorg. Chem.* **1999**, *38*, 218–228.
[24] W. B. Zhou, Z. C. Dong, J. L. Song, H. Y. Zeng, R. Cao, G. C. Guo, J. S. Huang, J. Li, *J. Cluster Sci.* **2002**, *13*, 119–136.
[25] Q. F. Zhang, Z. Yu, A. Rothenberger, D. Fenske, W. H. Leung, *Inorg. Chim. Acta* **2007**, *360*, 1568–1574.
[26] J. Diaz, M. P. Gamasa, J. Gimeno, A. Tirpicchio, M. T. Camellini, *J. Chem. Soc., Dalton Trans.* **1987**, 1275–1278.
[27] Q. F. Zhang, S. S. S. Raj, H. K. Fun, X. Q. Xin, *Chem. Lett.* **1999**, 619–620.
[28] M. A. Ansari, C.-N. Chau, C. H. Mahler, J. A. Ibers, *Inorg. Chem.* **1989**, *28*, 650–654.
[29] M. A. Ansari, C. H. Mahler, G. S. Chorghade, Y.-J. Lu, J. A. Ibers, *Inorg. Chem.* **1990**, *29*, 3832–3839.
[30] V. W.-W. Yam, K. K. W. Lo, K. K. Cheung, *Inorg. Chem.* **1996**, *35*, 3459–3462.
[31] C. W. Liu, I. J. Shang, J. C. Wang, T. J. Keng, *Chem. Commun.* **1999**, 995–996.

 © 2007 Wiley-VCH Verlag GmbH & Co. KGaA, Weinheim

[32] Q. F. Zhang, M. T. Bao, M. C. Hong, R. Cao, Y. L. Song, X. Q. Xin, *J. Chem. Soc., Dalton Trans.* **2000**, 605–610.
[33] C. C. Christuk, J. A. Ibers, *Inorg. Chem.* **1993**, *37*, 5105–5108.
[34] M. Sheik-Bahae, A. A. Said, T. H. Wei, D. J. Hagan, E. W. van Stryland, *IEEE J. Quantum Electron.* **1990**, *26*, 760–769.
[35] M. Sheik-Bahae, A. A. Said, E. W. van Stryland, *Opt. Lett.* **1989**, *14*, 955–957.
[36] S. Shi, Z. Lin, Y. Mo, X. Q. Xin, *J. Phys. Chem.* **1996**, *100*, 10696–10701.
[37] Z. R. Chen, H. W. Hou, X. Q. Xin, K. B. Yu, S. Shi, *J. Phys. Chem.* **1995**, *99*, 8717–8721.
[38] H. G. Zheng, Y. Xiao, Y. X. Wang, M. H. Ma, Y. Cai, A. Usman, H. K. Fun, Y. L. Song, X. Q. Xin, *Inorg. Chim. Acta* **2003**, *351*, 63–68.
[39] M. K. M. Low, H. W. Hou, H. G. Zheng, W. T. Wong, G. X. Jin, X. Q. Xin, W. Ji, *Chem. Commun.* **1998**, 505–506.
[40] C. Zhang, Y. L. Song, B. M. Fung, Z. L. Xue, X. Q. Xin, *Chem. Commun.* **2000**, 843–844.
[41] C. Zhang, Y. L. Song, Y. Xu, H. K. Fun, G. Y. Fang, Y. X. Wang, X. Q. Xin, *J. Chem. Soc., Dalton Trans.* **2000**, 2823–2829.
[42] C. Zhang, Y. L. Song, F. E. Kühn, Y. X. Wang, X. Q. Xin, W. A. Herrmann, *Adv. Mater.* **2002**, *14*, 818–822.
[43] S. C. O'Neal, J. W. Kolis, *J. Am. Chem. Soc.* **1988**, *110*, 1971–1972.
[44] G. J. Kubas, *Inorg. Synth.* **1996**, *28*, 68–70.
[45] F. T. Wang, J. Najzionek, K. L. Leneker, H. Wasserman, D. M. Braitsch, *Inorg. Synth. Met.-Org. Chem.* **1978**, *8*, 119–125.
[46] G. M. Sheldrick, *SHELXTL-97 Version 5.1*, Software Reference Manual, Bruker AXS, Inc., Madison, Wisconsin, USA, **1997**.

Received: November 25, 2006
Published Online: April 4, 2007

 © 2007 Wiley-VCH Verlag GmbH & Co. KGaA, Weinheim